



Download PDF

Export

Search ScienceDirect



Advanced search



Chemical Engineering Science

Volume 113, 3 July 2014, Pages 35–44

Effect of ultrasound on mass transfer during electrodeposition for electrodes separated by a narrow gap

S. Coleman  , S. Roy

[+ Show more](#)

<http://dx.doi.org/10.1016/j.ces.2014.03.026>

Open Access funded by Engineering and Physical Sciences Research Council

Under a Creative Commons [license](#)

Highlights

- Mass transfer during electrodeposition using side-on ultrasonic agitation
- Narrow electrode gaps and limitations of the limiting current technique
- Mass transfer correlation is developed for the side-on system for a narrow gap
- Developed and fully turbulent flows were found for narrow and large gaps
- Distortions in polarization data is caused by close placement of ultrasonic probe

Abstract

This work reports an investigation on mass transfer by ultrasound agitation during electrodeposition on electrodes separated by a narrow inter-electrode gap. Experiments were performed to identify the mass transfer limiting current. The limiting current density was used to calculate mass transfer boundary layer thickness. The results were used to develop mass transfer correlations. Experiments were carried out on parallel copper discs which were positioned at gaps of 1, 0.5 and 0.15 cm. The distance between the ultrasonic probe and electrodes was varied between 3 and 1 cm. The polarization data showed clear limiting current plateaux when the distance

electrodes was larger, however significant distortions were observed when the electrode spacing was 0.15 cm. It was found that lower ultrasound powers of 9–18 W/cm² provided better agitation at narrower electrode gaps than powers exceeding 18 W/cm². Statistical correlations showed that in this system, developing turbulence occurs for larger electrode spacing, whereas for narrow electrode gaps fully turbulent correlations were obtained. A 2-D current distribution model showed that potential distortions observed in the polarisation data were caused by the close placement of the probe to the two parallel electrodes.

Keywords

Electrodeposition; Ultrasonic agitation; Enface Technique; Mass transfer; Limiting current

1. Introduction

Microfabrication has a variety of applications, including fabrication of MEMS and micro-optic systems ([Franssila, 2010](#) and [Madou, 2012](#)). The widespread use of micro-products has led to the search for new microfabrication processes ([Dorai et al., 2009](#), [Samarasinghe et al., 2006](#), [Whitaker et al., 2005](#) and [Yu et al., 2006](#)). One such method is an electrochemical process, called EnFace ([Roy, 2007](#)). The process allows to selectively etch or plate metal at the microscale, using a patterned tool plate in close proximity to the substrate surface, when a voltage or current is passed between them. Experimentally, it was shown that copper patterns ranging between 5 and 100 μm were successfully etched ([Schönenberger and Roy, 2005](#)) or deposited ([Wu et al., 2005](#)) in a vertical flow-by system.

Since the technique required inter-electrode gaps of less than 500 μm, forced convection flow was needed to assist with species transport to and from the electrode surfaces. Furthermore, modelling studies showed that both forced convection flow velocity and electrode gap was a crucial parameter in controlling the ability of pattern transfer ([and Roy, 2008](#) and [Wu et al., 2011](#)). Due to the issues associated with sc

cell, the ability to etch or plate at the microscale was also investigated using beaker-type geometry. However, implementing Enface in a non-agitated restricted the mass transfer of ionic species within the inter-electrode gap (Roy, 2011). This investigation established that a method which directs a narrow gap was required.

It is well known that a diffusion layer forms at an electrode surface; if the reaction is out for short periods of time when diffusion is the dominant transport mechanism, the classical equations developed by Cottrell (1903) and Sand (1901) may be used. If the reaction results in a movement of ions in the bulk leading to natural convection, then laminar or turbulent correlations for free convection, such as those of Wagner (1949) and (1-b) (Fouad and Ibl, 1960) respectively, may be used.

Alternatively, agitation can be provided via forced convection flow and correlations such as Sherwood number correlations, such as Eq. (2) can be used (Tobias and

For the case of turbulent flow between two parallel plates the general Sherwood correlation is

While these equations have been used extensively (Wragg, 1971 and Wragg, 1967), they are valid only when the two electrodes are sufficiently far from each other so that interaction of boundary-layer does not take place.

In fact, few mass transfer correlations exist for forced convection between electrodes are separated by a narrow gap. Although several studies on electrodeposition growth (Kuhn and Argoul, 1995), surface adsorption (Texier et al., 1998) and electrochromism (Compton et al., 1996b and Tolmachev et al., 1996) have been carried out in a horizontal channel cell with a thin gap, this system has never been used for electrodeposition purposes. Where steady state electrochemical deposition has been performed, it has been shown that electrochemical reactions within narrow gaps exhibit concentration instabilities in material transport (Rosso et al., 2002 and Zelinsky and Pirogov, 2009). For example, silver deposition onto silver electrodes separated by a narrow gap in a 0.01 M AgClO_4 electrolyte showed oscillations in the transfer of ions due to the presence of boundary layers near the electrode surface (Zelinsky and Pirogov, 2009). Electrodeposition from 0.1 M CuSO_4 at parallel plates with an inter-electrode gap of 8 mm also exhibited concentration instabilities as the mass transport limit was approached (Rosso et al., 2002). Both these studies confirmed that such thin gap cells are not suitable for electrodeposition due to mass transfer limitations.

Ultrasonics (US) is a forceful form of agitation which can improve stirring in electrochemical systems (Compton et al., 1996a and Walton et al., 1995). An ultrasonic transducer is a vibrating solid that can induce ultrasound waves through a solution which causes cavitation. It is suggested that cavitation phenomena contributes to the enhanced mass transfer during stirring (Compton et al., 1996a, Maisonhaute et al., 2001, Mason and Lorimer, 2002, Ohsaka et al., 2010, Ramachandran and Saraswathi, 2009, Richardson et al., 2009, Walton et al., 1995 and Yeager and Hovorka, 1953). Much of the research has established the improvement of mass transfer in electrodes which are far from the mass transport limit (Compton et al., 1996a, Lorimer et al., 1996 and Marken et al., 1996 and Saraswathi, 2009), but no information is available for cases where the mass transport limit is approached in the gap between parallel plates.

The effect of US agitation has been most extensively studied by probes oriented normal to the working electrode surface (Compton et al., 1996a, Marken et al., 1996 and Ramachandran and Saraswathi, 2009), illustrated in Fig. 1(a).

orientation, with a reduction of δ at the working electrode for example demonstrated the importance of the distance from the probe tip to the center of the electrode surface (d_p), showing that the limiting current (i_{Lim}) is approximately proportional to d_p^{-1} (Marken et al., 1996). This was attributed to the narrower jet of flow close to the tip compared to distances further away (Marken et al., 1996), thereby increasing the rate of mixing at the electrode surface as the tip is brought closer to it. The effect of power intensity on mass transfer has also been investigated (Compton and Lorimer et al., 1996 and Ramachandran and Saraswathi, 2009). For instance, in the study of a $K_4Fe(CN)_6$ redox reaction at a glassy carbon electrode, varying the power intensity showed that the diffusion layer thickness (δ) is approximately proportional to $P^{-1/2}$ (Compton et al., 1996a). These investigations illustrated the importance of choosing appropriate parameters to influence mass transfer in electrochemical systems.

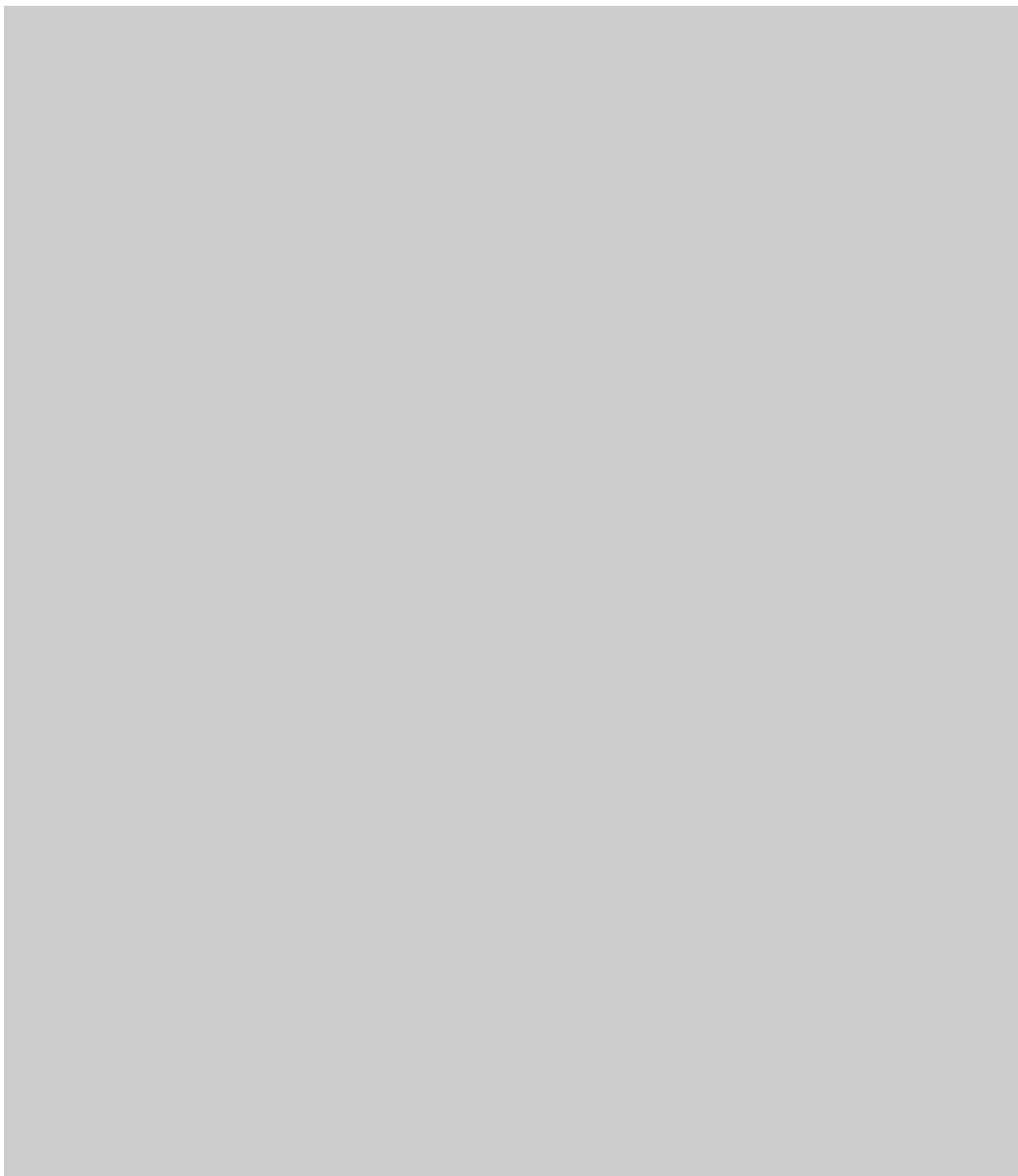


Fig. 1.
US probe orientations relative to an electrode. (a) face-on; (b) side-on; and (c) side-on v
gap. Adapted from [Marken et al. \(1996\)](#).

To these authors' knowledge only one investigation has been carried out

ultrasound variables in the side-on geometry (Eklund et al., 1996), display This investigation studied the effect of the 'side-on' probe on the mass transport and oxidation of ferrocene at a platinum plate electrode. The researchers developed a theoretical analysis based on earlier forced convection systems where they used the electrodes (Levich, 1962). They established that agitation conditions could be modeled using such a model, and that the diffusion layer across the surface of the electrode was uniform and had thicknesses of 10–12 μm at the downstream edge of the probe (Eklund et al., 1996).

At this point the effectiveness of US agitation to enable mass transport within narrow electrode gaps, as illustrated in Fig. 1(c), has remained unexplored. In this work, we aim to quantitatively assess the effect of US agitation on mass transfer during metal deposition in a system with a combined geometry of a 'side-on' probe and a narrow inter-electrode gap. A well-established limiting current technique, widely used for determining material transport, is employed to determine the thickness of mass transfer boundary layers. The electrochemical system is copper deposition from a CuSO_4 solution, where flow instabilities have been encountered (Rosso et al., 1996). We have measured the limiting current for copper deposition with and without US agitation. Limiting currents have been used to calculate the mass transfer boundary layer thickness and Sherwood number correlations have been developed. Experiments were carried out using a small cell where parallel electrodes at gaps of 1, 0.5 and 0.15 cm were placed. The gap between the US probe and electrodes has been varied between 0.5 and 1.5 cm. The usefulness of utilizing the limiting current method, which is often used to determine mass transfer boundary layer thickness during electroplating, is being examined, particularly for the case of narrow electrode geometries.

2. Theory

It is suggested that the flow regime from an ultrasound probe tip is similar to the flow from a pipe of the same diameter (Marken et al., 1996). Furthermore, Marken et al. (1996) proposed that the flow of ultrasound waves over an electrode surface using a 'side-on' probe is analogous to flow over a plate. Based on this assumption, the

used an analysis proposed by [Levich \(1962\)](#) for forced convection. They describe the limiting current at an electrode when such a forced US agitation is used in a side-on arrangement ([Eklund et al., 1996](#)).

In Eq. (4), F , D , c_b and ν are the Faraday constant, diffusion coefficient, bulk concentration of reacting species and the kinematic viscosity respectively. The parameter r is the radius of the electrode, and the parameter x is the distance along the length of the electrode edge closest to the probe. In Eq. (4) h_0 is the distance between the leading edge of the momentum and the concentration boundary layers. The limits of the integration are from h_0 to $h_0 + 2r$ since the deposition reaction occurs at the metal surface (c.f. [Eklund et al., 1996](#)).

The only unknown parameter in the equation is U , the velocity of the flow far from the electrode surface. For US agitation, U is related to the ultrasound power and the solution velocity at a large distance from the plate. The effect of bringing the probe closer to the electrode is governed by changing the parameter ' d_p ', which is defined as the distance from the centre of the electrode to the US probe tip. It has been shown in earlier experiments that a distance between the probe and electrode of >3 cm is sufficiently far from the electrode surface for Eq. (4) to hold ([Compton et al., 1996a](#) and [Eklund et al., 1996](#)).

[Eklund et al. \(1996\)](#) carried out experiments using a 20 kHz probe placed 34 mm away from a platinum plate electrode where ferrocene was oxidised electrochemically. Experimentally measured limiting currents were used to determine the value of U using Eq. (4) at various ultrasound intensities. This analysis showed that the limiting current is proportional to US power, which is displayed in [Fig. 2](#). This proved that the flow model was a reasonable model for this side-on probe system.



Fig. 2.

A graph of U (best-fit value) obtained from the data (black square) published by Eklund distance between the probe and the centre of the electrode was 34 mm.

3. Methodology

Experiments were carried out in a 500 ml cylindrical PVC cell with two pol discs 1 cm in diameter acting as a cathode and anode, and faced each of an electrode gap (Fig. 3). The distance between the electrodes was altered 1 cm with the use of screw gauges on each electrode holder. The reference copper wire wrapped in PTFE tape with only the tip exposed, placed approx from the cathode surface, above and to the side of the electrode gap. Cop reference electrode in acidified CuSO_4 electrolytes, and has been used for measurement of polarisation data (Meuleman and Roy, 2003 and Roy et al; electrolyte solution used was an acidic electrolyte of 0.1 M CuSO_4 +0.1 M



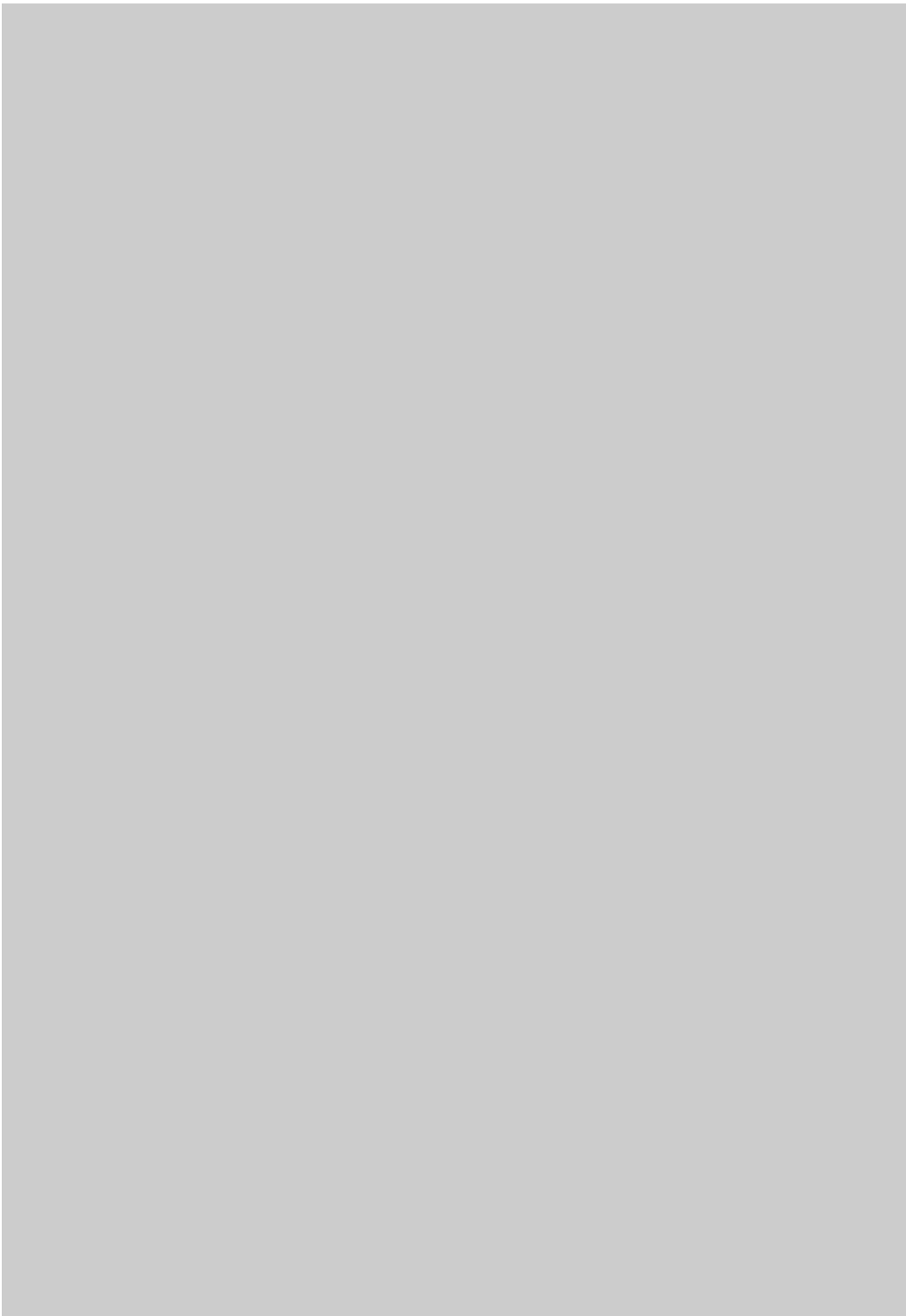


Fig. 3.

(a) Experimental set-up of the electrochemical cell used in this work with ultrasound probe above the narrow electrode gap; (b) position of probe in solution above the working electrode variable parameter d_p . (c) Side view of placement of probe, with concentration (c) and flow profiles demonstrating the development of the momentum and concentration boundary

An *Eco Chemie Autolab Potentiostat (PGSTAT30)* was used to apply linear potential scans and *NOVA 1.7* software was used to input scan settings and response data. The ultrasonic equipment used was a *SONICS Vibra-Cell Processor* connected to a 20 kHz ultrasound probe with a 1.3 cm diameter and was operated within a power range of 9–29 W/cm². The probe was positioned in a side-on orientation (Fig. 3), with $d_p=1.5–3$ cm. The probe tip was positioned 0.4 cm above the solution by 0.4 cm for every probe–electrode distance.

The limiting current technique is based on the identification of limiting current from standard electrode polarisation data. For any electrochemical reduction reaction, the current changes with potential, until it reaches the region where the reaction is mass transfer controlled. In this region the current becomes independent of the applied potential, and a current plateau is observed in the polarisation data. This plateau current, termed as the mass transfer limiting current, is related to the diffusion layer thickness. The limiting current density can be used to calculate the diffusion layer thickness:

$$i_{lim} = \frac{zFD(c_b)}{\delta}$$

In Eq. (5), z is the charge on the reacting species, D is the diffusivity of the reacting species and δ is the diffusion layer thickness. The value of δ was calculated using the limiting current and concentration stated in the experimental section and a diffusion coefficient of 7.07×10^{-6} cm²/s calculated using equations from [Fenech and Tobias \(1998\)](#).

The values of δ values calculated from the limiting current experiments were used to develop Sherwood number correlations. Sh numbers were calculated by $Sh=L/\delta$ where L is the characteristic length, in this case $2r=1$ cm, where r is the radius of the electrode.

electrode (c.f. [Fig. 8](#)). The Sc number was calculated by $Sc=v/D$ where a kinematic viscosity (ν) of $1.004 \times 10^{-2} \text{ cm}^2/\text{s}$ was used and the diffusivity (D) was the same as used in the limiting current calculations. The value of Re was based on the diameter (d_H), which was used to calculate the equivalent diameter (d_e). The procedure is stated in the [Appendix](#).

4. Results

[Fig. 4a–c](#) show the linear polarization scans for copper deposition at the cathode using US agitation. Limiting current plateaux are observed as expected due to mass transport limitation for copper deposition, although the data for lower probe–electrode distances and narrow inter-electrode gaps exhibit smaller plateau regions, resulting in a difficulty in measuring the limiting current density (i_{Lim}). This measurement was also made more difficult due to current fluctuations caused by cavitation bubble oscillations and micro-jetting resulting in current peaks, which have been previously observed in side-on ([Eklund et al., 1996](#)) as well as face-on ([Compton et al., 1996a](#) and [Marken et al., 1996](#)) and probe arrays ([Fig. 4b](#) and [c](#), where probe–electrode distance or inter-electrode gap are small). Hydrogen discharge potentials apparently occur at lower potentials, which makes the determination of limiting current difficult.

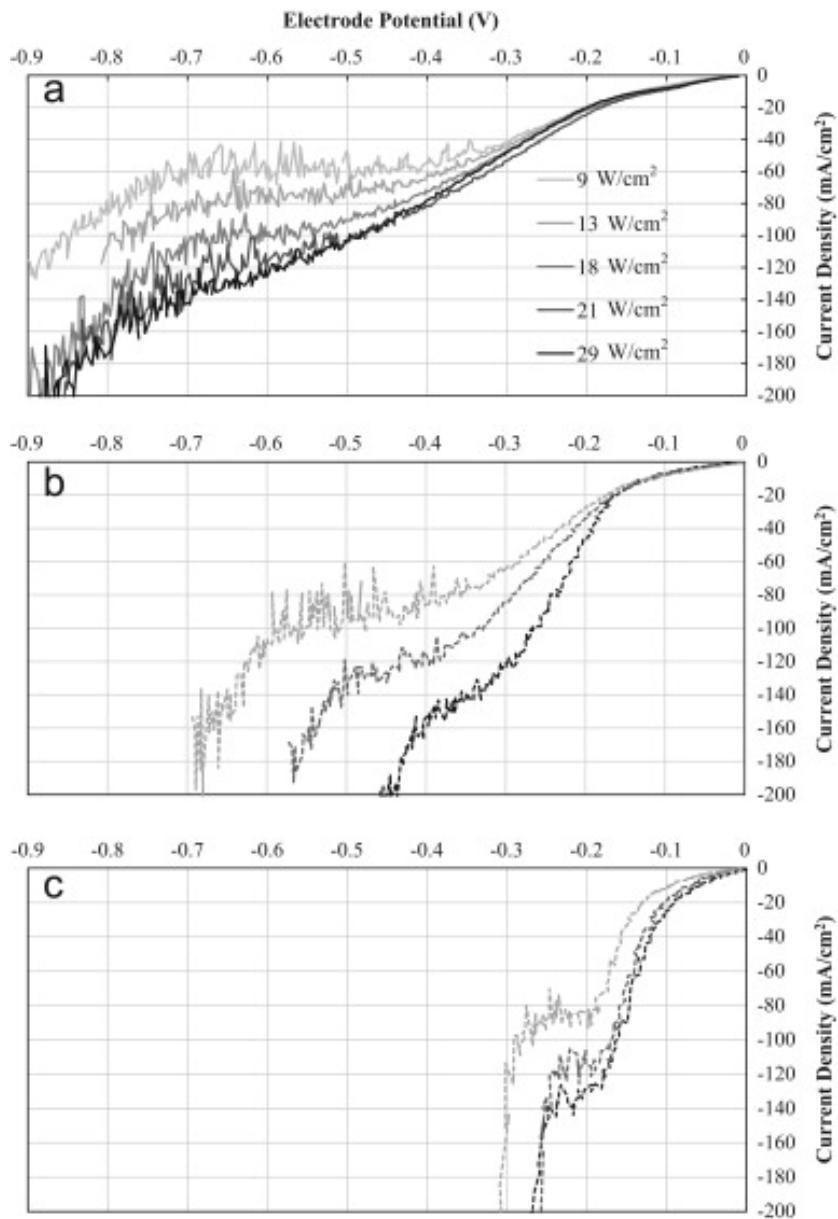


Fig. 4. Linear Potential scans with a 0.1 M CuSO_4 +0.1 M H_2SO_4 electrolyte; Scan Rate=5 mV/s; ultrasound intensities (9–29 W/cm^2), $h_e=1$ cm; $d_p=3$ cm. (b) $h_e=0.5$ cm; at varying d_p (solid grey), 2 cm (dashed grey) and 1.5 cm (dashed black) at fixed p of 18 W/cm^2 . (c) $h_e=0.5$ cm; ultrasound conditions as for 'b' and varying d_p at distances of 3 cm (dashed light grey), and 1.5 cm (dashed black).

The values of i_{Lim} for an inter-electrode gap of 1 cm (Fig. 4a) are in the range of -130 mA/cm^2 . This value is significantly greater than the i_{Lim} value measured under silent conditions, which was recorded at -10.5 mA/cm^2 respectively. Ultrasound agitation provided by ultrasound significantly increases the rate of mass transport towards the substrate. This enhancement in limiting current density with ultrasound intensity has been previously reported in sonoelectrochemical investigations using a parallel-plate geometry (Eklund et al., 1996) and face-on geometry (Compton et al., 1996a and Ramachandran and Saraswathi, 2009).

Fig. 4b displays linear potential scans under ultrasound conditions for a narrow inter-electrode gap and varying probe–electrode distances. The value of i_{Lim} at an inter-electrode gap of 0.5 cm is approximately 90, 122 and 140 mA/cm^2 for the probe–electrode distances of 3, 2 and 1.5 cm respectively illustrating the increase in mass transport as the probe is brought closer towards the electrode, evident in previous ultrasound studies where the probe–electrode distance is varied (Compton et al., 1996a and 1996; Ramachandran and Saraswathi, 2009). It is suggested that this is due to the presence of a higher flow velocity at shorter distances from the probe tip (Compton et al., 1996).

Fig. 4c displays linear potential scans under ultrasound conditions for a narrow inter-electrode gap and varying probe–electrode distances. The value of i_{Lim} is virtually unchanged when the electrode spacing is decreased from 0.5 to 0.15 cm demonstrating that ultrasound is an effective form of agitation even for narrow inter-electrode gaps. However, the polarisation data are significantly different when using a narrow inter-electrode gap, i.e. 0.15 cm, being distorted, with a very small plateau region.

The i_{Lim} values from polarization data were used with Eq. (4) to calculate the thickness of the diffusion layer (δ) at the cathode at varying US powers and probe–electrode distances of 1 cm (large) and 0.15 cm (small), displayed in Fig. 5. These δ values and layer thickness are calculated for a probe–electrode distance of 3 cm, which

deemed to be sufficiently far from the electrode surface.

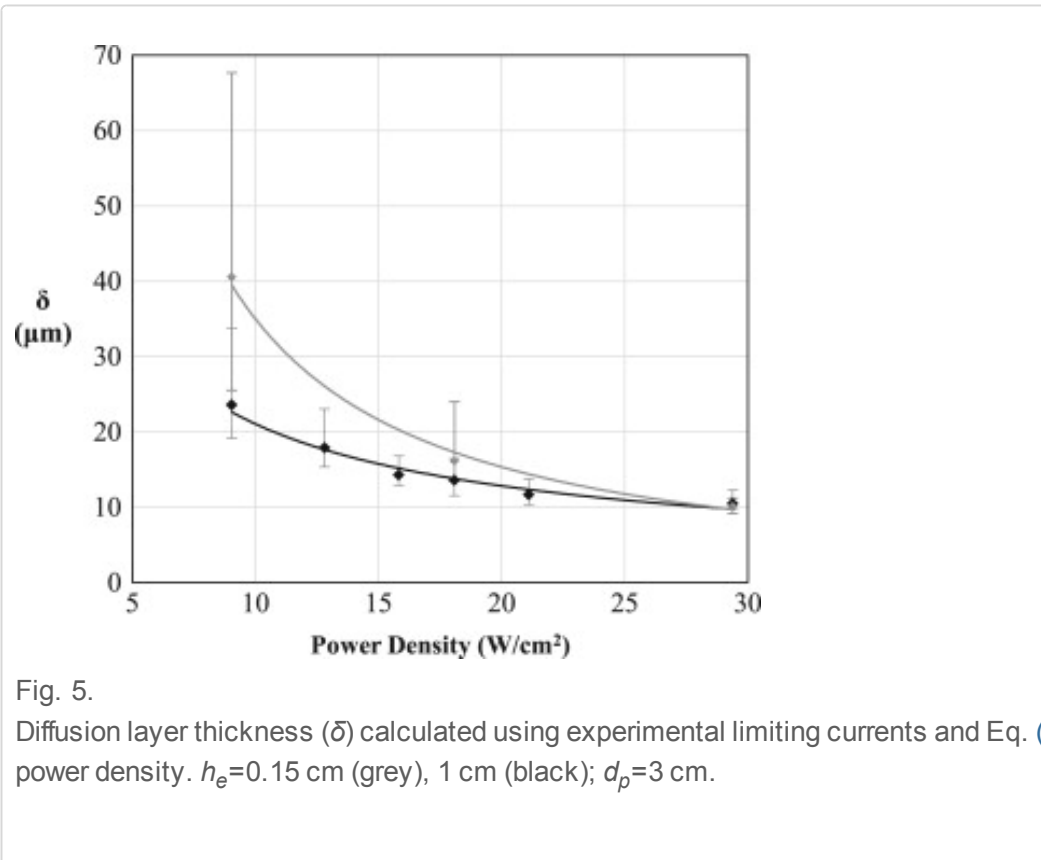


Fig. 5. Diffusion layer thickness (δ) calculated using experimental limiting currents and Eq. (5) power density. $h_e=0.15$ cm (grey), 1 cm (black); $d_p=3$ cm.

As expected, the boundary layer is larger at lower US intensities compared to higher intensities for the case of the constant electrode separation of 1 cm. Narrowing the electrode gap from 1 cm to 0.15 cm increases the δ due to constriction of the flow. Interestingly, the decrease in the thickness of the boundary layer for the narrower gap is higher, as is seen from the data at US intensities higher than 10 W/cm^2 . Finally, for both electrode gaps, a minimum diffusion layer thickness (δ_{min}) is reached as the ultrasound power is raised. It has been suggested that this is due to the limiting conversion of ultrasound energy to turbulent liquid flow (Markovskii, 1965). In all cases shown in Fig. 4a–c, the values of δ achieved with US are more than twice those under silent conditions, which shows the usefulness of such agitation.

In order to examine more deeply into the mechanism of US agitation at the surface, Sherwood number correlations were developed. For this purpose, the flow velocity, U , far away from the electrode is required. The flow velocity (U) of ultrasound waves flowing between the electrodes at different ultrasound powers was estimated using the relationship formulated by Eklund et al. (1996), which is shown in Fig. 2. The value of Reynolds number, Re , was calculated using $Re=(Ud_p/\nu)$, where U is the flow velocity shown in Fig. 2. The Re numbers for the range of ultrasound powers used in the experiments were found to be approximately 700–2000 and 2700–7400 for the small and large gaps, respectively, as shown in Table 2 in Appendix.

Table 1.

Calculated change in potential at the cathode surface for varying electrode gaps and probe distances.

Change in probe distance, d_p (cm)	Change in electrode gap, h_e (cm)	Change in potential at cathode (V)
3–1.5	1 (constant)	+0.130
3–1.5	0.15 (constant)	+0.085
3 (constant)	1–0.15	+0.135
1.5 (constant)	1–0.15	+0.090
3 to 1.5	1–0.15	+0.220

Sherwood–Schmidt–Reynolds numbers correlations for copper deposition were developed for electrode gaps of 0.15 cm and 1 cm, shown in Fig. 6. The line of best-fit correlations displayed in Eqs. (6) and (7) for electrode gaps of 1 cm and 0.15 cm, respectively.

$$Sh = 1.7 \times 10^{-3} \left(Re Sc \frac{d_e}{L} \right)^{0.82}$$

$$Sh = 9 \times 10^{-6} \left(Re Sc \frac{d_e}{L} \right)^{1.38}$$

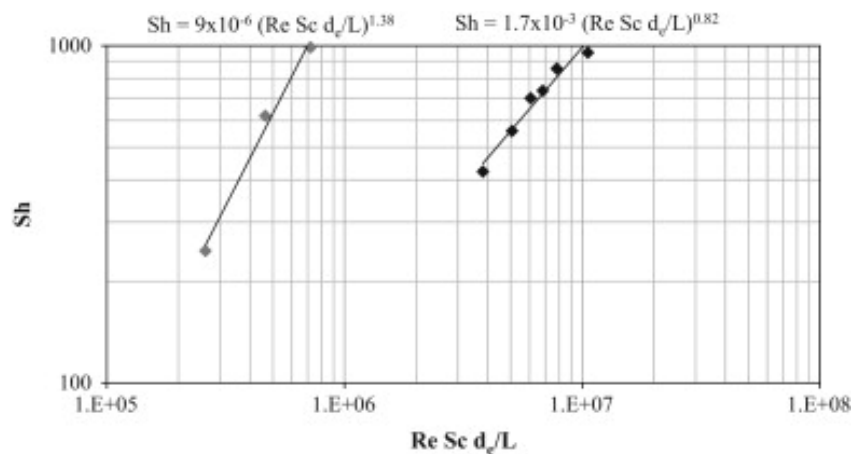


Fig. 6. Mass transfer correlations using US agitation. Data shown for US power 18 W/cm^2 and distance of 3 cm, where the US source is far away from the electrode. Inter-electrode gap is 1 cm (black) and 3 cm (grey).

These correlations can be compared against standard mass transfer correlations for forced convection flow between two parallel electrodes, displayed in Eq. (6). For the 1 cm electrode gap is ~ 0.8 , showing the onset of turbulent flow. However, turbulent flow becomes fully developed when the electrode gap is narrower, as illustrated by the value of b of ~ 1.4 in Eq. (7). It is suggested that this is possible due to the formation of eddies at the top of the narrower gap, which could occur when the interaction of ultrasound waves come into contact with the top section of the electrode.

It is significant that the Sh correlation shows fully developed turbulence for which means that the efficacy of US is higher even though the Re values are low. For example, at 29 W/cm^2 , the Re for the small and large gap is 2000 and 7400, respectively, but the value of δ is virtually the same. The turbulence in the narrower gap is due to the interaction between the US waves and the edges of the parallel electrodes, leading to eddy formation, which needs to be investigated further.

5. Discussion

A noticeable issue in this work was the difficulty in detecting a limiting current when the electrodes were placed close to each other or when the distance between electrodes was lowered. Although current oscillations have been observed in previous investigations (Compton et al., 1996a, Eklund et al., 1996 and Marken et al., 1996), for both side-on and face-on geometries, there is less information on distorted current data during electrochemical reactions. Marken and Compton (1996) have suggested that current can flow to the US probe itself, since it is metallic, and has also suggested ways of obviating this problem; including bipotentiostatic control and electrically insulating the probe. However, bipotentiostats are not used in industry and therefore cannot be used for industrial applications, and electrically insulating the probe may lower the ultrasound signal. Polarisation data of other researchers have also shown that limiting currents are often observed during US agitation (Reisse et al., 1994). In our case, it can be seen that the plateau region is very small. This means that the limiting current technique has only limited applicability for measuring mass transfer limitations for electrochemical systems using US.

In order to examine more deeply into the apparent distortion in potential measurements, further analysis was carried out. There is a possibility that the probe is acting as a second working electrode relative to the electrodes. However, Marken and Compton (1996) suggests that the ultrasound probe placed within an electrolyte solution of an electrochemical cell should be a second working electrode; therefore the surface of the probe was modelled as a cathode. A primary current distribution model of copper electrodeposition was developed using a commercial electrodeposition software, EISyca (EISy, SA) using a two-electrode model of the cell in Fig. 3. The software was used to determine if the potential for hydrogen evolution region begins could shift from -0.6 V to -0.3 V as the probe distance decreased from 0.5 to 0.15 cm at a probe distance of 3 cm, as was observed in the polarisation experiment shown in Fig. 4.

The calculation used for the model assumed that there is a uniform concentration of ions in the solution and also constant electrolyte conductivity. The well-known equation for the flux of an ionic species k (N_k) was used, shown in Eq. (8).

$$N_k = -D_k \nabla c_k + c_k v - z_k u_k F c_k \nabla \phi$$

where u_k is the mobility of species k ($\text{cm}^2 \text{mol}^{-1} \text{s}$) and $\nabla \phi$ is the potential. The accumulation of species k can be expressed as the equation shown

$$\frac{\partial c_k}{\partial t} = -\nabla \cdot N_k + R_k$$

where R_k is the production rate of species k (mol/s). A more convenient equation can be written as Eq. (10), derived by substituting Eq. (8) into Eq. (9)

$$\frac{\partial c_k}{\partial t} + v \cdot \nabla c_k = z_k F \nabla (u_k c_k \nabla \phi) + \nabla (D_k \nabla c_k), \quad k = 1, \dots, n$$

The velocity of an incompressible fluid flow in electrochemical systems is well-known Navier–Stokes equation, with constant density and viscosity

$$\nabla \cdot v = 0$$

The electric potential (ϕ) in an electrochemical system can be expressed by the Poisson equation, shown in Eq. (12). However, this can be replaced with the electroneutrality expression in Eq. (13) due to the condition that the bulk electrolyte solution is electrically neutral.

where ϵ is the dielectric constant of the solution (Farad/m). The current density can be described by Eq. (14). If N_k is substituted by Eq. (8), then the current density can be expressed in terms of diffusion, convection and migration. If the conductivity is taken into account (Eq. (13)), along with the condition of electroneutrality (Eq. (13)), the current density can be given by Eq. (16).

For steady-state conditions, Eq. (10) can be omitted. If there is a continuous solution, it can be assumed that convection is dominant and concentration is omitted, therefore Eq. (10) can be simplified to Eq. (17), the well-known Laplace equation. This means that the current density can be expressed as Eq. (18).

$$\sigma \nabla^2 \phi = 0$$

$$i = -\sigma \nabla \phi$$

This model is solved using the Boundary Element Method in EISyca, using boundary conditions that the current density at each point at the insulating walls of the surface of the solution is zero. This means that the current flows to the electrodes in the case of the anode, cathode as well as the US probe placed in solution.

where y denotes the normal distance from the surface.

A constant temperature of 293 K was used and the electrolyte conductivity was 59.8 mS/cm. The dimensions of the US probe were modelled as a rectangle with a width of 1.3 cm and a height of 0.4 cm respectively, placed above the electrode gap. The same dimensions were used on both the cathode and anode, 120 elements on the surface of the electrodes and 30 elements on the side of the probe. The convergence of the current density calculation was achieved when the current residual reached a value < 0.001 mA/cm² and the calculation was completed within 6 iterations (at a maximum of 20 iterations).

Typical results from the modelling analysis are presented in Fig. 7. The potential distribution is shown in Fig. 8.

electrode gaps of 1 cm and 0.15 cm with the ultrasound probe at probe–electrode distances of 3 cm and 1.5 cm are shown in the figure. The results show the presence of a large metallic probe, significant distortion in the potential field. When electrodes are brought closer together or when the probe is brought close to the electrodes the distortion in the field is greater and current begins to flow towards the probe surface proposed by Marken and Compton (1996). This resulted in copper deposition on the probe surface, observed during our polarization experiments. The current flow from the anode to the probe surface meant that smaller current densities were calculated across the section of the cathode surface in the modelling. This would therefore be the cause of the deposit thickness non-uniformity along the cathode length.





Fig. 7.
Potential isolines within the electrochemical cell with an ultrasound probe placed in the cell with cathode (left) and anode (right). Potential applied = -0.1 V. (a) $h_e = 1$ cm; $d_p = 3$ cm. (b) $d_p = 1.5$ cm.

The change in potential at the cathode at different probe distances and electrode geometries is displayed in [Table 1](#). Interestingly, the cathode potential can shift by 0.085 V in the positive direction depending on the proximity of the US probe and the two electrodes. This shift in potential is of a similar magnitude to the shift in potential observed experimentally in [Fig. 4](#), which explains the differences in polarisation data for different electrode geometries. Both narrowing the electrode gap and lowering the flow rate result in potential distortions which shorten the current plateaux, and also reduce the current flow through the probe. This measured limiting current is therefore inaccurate due to the distance between the probe and the electrodes. Our modelling data show that the total current flowed to the probe for the smallest probe to electrode distance is significantly lower than the limiting current technique. Our findings therefore show that within very constricted geometries, the empirical limiting current technique may be limited.

Table 2.

Calculated Reynolds numbers at varying powers for two different electrode gaps, with flow rate, obtained from [Fig. 2](#).

Electrode gap (cm)	Power (W/cm ²)	Velocity, <i>U</i> (cm/s)	<i>Re</i>
1	9	27	2686
	18	48	4795
	29	75	7430
0.15	9	27	701
	18	48	1251
	29	75	1938

6. Conclusions

The effect of a side-on ultrasound probe on the mass transfer during copp

narrow inter-electrode gaps was investigated. The limiting current technique determine the diffusion layer thickness, which were then used to determine correlations. It was found that ultrasonic agitation significantly improved the ability to increase limiting currents by a factor of 10.

Ultrasound powers of 9–18 W/cm² were found to provide more effective stirring than expected, stirring at the electrode surface increased as the US probe was brought closer to the electrodes. Sherwood correlations showed that turbulence was present near the electrode surface when a side-on probe is used. For large electrode spacing the developing turbulence was observed, whereas for narrow electrode spacing turbulent correlations were obtained.

Polarisation data for copper deposition were found to be distorted when the probe was brought closer to the electrodes, and when the anode and cathode were in close proximity. A current distribution analysis showed that the distortion in polarisation was caused by the close placement of the metallic US probe to the two parallel electrodes. These findings hold implications for limiting current analyses used to study mass transport within narrow electrode gaps in a horizontal regime or within concentric cylindrical electrodes in close proximity to each other (Coeuret and Legrand, 1981), and other ultrasonic applications where the source of ultrasound has to be placed in close proximity to a substrate or work piece.

Nomenclature

ϕ	potential (V)
a	constant coefficient in Sherwood correlation
A	cross-sectional area of channel between the electrodes (cm ²)
b	exponent in Sherwood correlation
c	concentration (mol/cm ³)
d	distance (cm)

D	diffusivity (cm^2/s)
δ	diffusion layer thickness (cm)
h_e	electrode gap (cm)
ϵ	dielectric constant of the solution (Farad/m)
F	Faraday constant (96485 A s/mol)
Gr	Grashof Number (dimensionless)
h_0	distance between the leading edge of the momentum and the boundary layers (cm)
i	current density (mA/cm^2)
I	current (mA)
L	characteristic length (cm)
N	flux of species ($\text{mol}/\text{cm}^2\text{s}$)
ν	kinematic viscosity (cm^2/s)
p	ultrasound power intensity (W/cm^2)
σ	conductivity (S/m)
r	radius (cm)
Re	Reynolds Number, dimensionless
R	production rate (mol/s)
Sc	Schmidt number, dimensionless
Sh	Sherwood number, dimensionless
t	time (s)
U	limiting solution velocity at a larger distance from the plate (cm)

u	mechanical mobility of species k ($\text{cm}^2\text{mol}/\text{J}\cdot\text{s}$)
w	electrode width (cm)
x	length along the electrode from the edge closest to the probe
z	charge of species

Subscripts

b	bulk
e	equivalent (diameter) (cm)
H	hydraulic (diameter) (cm)
k	species
Lim	Limiting
min	minimum
p	distance from probe tip to the centre of the electrode surface (
$sono$	in the presence of ultrasonic agitation

Acknowledgements

Simon Coleman acknowledges the studentship support by EPSRC, UK grant [EP/J500288/1](#). This work was supported by EU “MESMOPROC” Grant 3. Chemical Engineering workshop is acknowledged for cell fabrication.

Appendix

Reynolds number calculations

The electrode dimensions were simplified to 1 cm square electrodes for this analysis, shown in the schematic in [Fig. 8](#). The hydraulic diameter (d_H) was

the equation $d_H = 4A / (4r + 2h_e)$, where A is the cross-sectional area of the c
the electrodes, r is the radius of the electrode and h_e is the electrode gap.



Fig. 8.
Schematic of electrode gap for calculation of d_H with assumption of square electrodes.
length, A =cross-sectional area, h_e =electrode gap.

References

- [Coeuret and Legrand, 1981](#) F. Coeuret, J. Legrand
Mass transfer at the electrodes of concentric cylindrical reactors combining rotation of the inner cylinder
Electrochim. Acta, 26 (7) (1981), pp. 865–872
[Loading](#)
- [Compton et al., 1996a](#) R.G. Compton, J.C. Eklund, S.D. Page, T.J. Mason, D.J. Wall
Voltammetry in the presence of ultrasound: mass transport effects
J. Appl. Electrochem., 26 (1996), pp. 775–784
[Loading](#)
- [Compton et al., 1996b](#) R.G. Compton, J.G. Gooding, A. Sokirko
Chronoamperometry at Channel Electrodes: analytical theory of transient l electrodes

J. Appl. Electrochem., 26 (1996), pp. 463–469

Loading

[Cottrell, 1903](#) F.G. Cottrell

Residual current in galvanic polarization, regarded as a diffusion problem

Z. Phys. Chem., 42 (1903), p. 385

Loading

[Doraiswamy et al., 2009](#) A. Doraiswamy, T.M. Dunaway, J.J. Wilker, R.J. Narayan

Inkjet printing of bioadhesives

J. Biomed. Mater. Res. Part B: Appl. Biomater. J. Biomed. Mater. Res. Part B: Ap (2009), pp. 28–35

Loading

[Eklund et al., 1996](#) J.C. Eklund, F. Marken, D.N. Waller, R.G. Compton

Voltammetry in the presence of ultrasound: a novel sono-electrode geome

Electrochem. Acta, 41 (9) (1996), pp. 1541–1547

Loading

[Fenech and Tobias, 1960](#) E.J. Fenech, C.W. Tobias

Mass transfer by free convection at horizontal electrodes

Electrochim. Acta, 2 (1960), pp. 311–325

Loading

[Fouad and Ibl, 1960](#) M.G. Fouad, N. Ibl

Natural convection mass transfer at vertical electrodes under turbulent flow

Electrochimica Acta., 3 (1960), pp. 233–243

Loading

[Franssila, 2010](#) S. Franssila

Introduction to Microfabrication

(2nd ed.)Wiley, West Sussex (2010)

Loading

[Kuhn and Argoul, 1995](#) A. Kuhn, F. Argoul

Diffusion-limited kinetics in thin-gap electroless deposition

J. Electroanal. Chem., 397 (1–2) (1995), pp. 93–104

Loading

[Levich, 1962](#) V.G. Levich

Physicochemical hydrodynamics

Prentice-Hall, New Jersey (1962), pp. 87–91

Loading

[Lorimer et al., 1996](#) J.P. Lorimer, B. Pollet, S.S. Phull, T.J. Mason, D.J. Walton, U. C

**The effect of ultrasonic frequency and intensity upon limiting currents at ro
stationary electrodes**

Electrochem. Acta, 41 (17) (1996), pp. 2737–2741

Loading

[Madou, 2012](#) M.J. Madou

Fundamentals of Microfabrication and Nanotechnology (3rd ed.), vol. 2, CRC Press

Loading

[Maisonhaute et al., 2001](#) E. Maisonhaute, P.C. White, R.G. Compton

Surface Acoustic Cavitation understood via nanosecond electrochemistry

J. Phys. Chem. B, 105 (48) (2001), pp. 12087–12091

Loading

[Marken and Compton, 1996](#) F. Marken, R.G. Compton

**Electrochemistry in the presence of ultrasound: the need for bipotentiostati
sonovoltammetric experiments**

Ultrason. Sonochem., 3 (1) (1996), pp. S131–S134

Loading

[Marken et al., 1996](#) F. Marken, R.P. Akkermans, R.G. Compton

**Voltammetry in the presence of Ultrasound: the limit of acoustic streaming
layer thinning and the effect of solvent viscosity**

J. Electroanal. Chem., 415 (1) (1996), pp. 55–63

Loading

[Mason and Lorimer, 2002](#) T.J. Mason, J.P. Lorimer

Applied Sonochemistry: Uses of Power Ultrasound in Chemistry and Process

Wiley, Weinheim (2002)

Loading

[Meuleman and Roy, 2003](#) W.R.A. Meuleman, S. Roy

Transient electrochemical processes during Cu-Ni deposition

Trans. Inst. Metal Finish., 81 (2003), pp. 55–58

Loading

[Nouraei and Roy, 2008](#) S. Nouraei, S. Roy

Electrochemical process for micropattern transfer without photolithography analysis

J. Electrochem. Soc., 155 (2) (2008), pp. D97–D103

Loading

[Ohsaka et al., 2010](#) T. Ohsaka, Y. Goto, K. Sakamoto, M. Isaka, S. Imabayashi, K.

Effect of intensities of ultrasound sonication on reduction of crack formation and surface roughness in iridium electrodeposits

Trans. Inst. Metal Finish., 88 (4) (2010), p. 206

Loading

[Ramachandran and Saraswathi, 2009](#) R. Ramachandran, R. Saraswathi

Sonoelectrochemical studies on mass transport in some standard redox systems

Rus. J. Electrochem., 47 (1) (2009), pp. 15–25

Loading

[Reisse et al., 1994](#) J. Reisse, H. Francois, J. Vandercammen, O. Fabre, A. Kirchchick

Maerschalk, J.-L. Delplanke

Sonoelectrochemistry in aqueous electrolyte: a new type of sonoelectrodeposition

Electrochim. Acta, 39 (1994), pp. 37–39

Loading

[Richardson et al., 1997](#) K.A. Richardson, P.A.J. de Groot, P.C. Lanchester, P.R. Birl

Towards the electrochemical manufacture of superconductor precursor films in an ultrasonic field

J. Electroanal. Chem., 420 (1) (1997), p. 22

Loading

[Rosso et al., 2002](#) M. Rosso, E. Chassaing, J.N. Chazalviel, Gobron

Onset of current driven concentration instabilities in thin cell electrodeposition at small inter-electrode distance

Electrochim. Acta, 47 (2002), pp. 1267–1273

Loading

[Roy et al., 2001](#) S. Roy, Y. Gupte, T.A. Green

Flow cell design for metal deposition at recessed circular electrodes and w

Chem. Eng. Sci., 56 (17) (2001), pp. 5025–5035

Loading

[Roy, 2007](#) S. Roy

Fabrication of micro- and nano-structured materials using mask-less proce

J. Phys. D: Appl. Phys., 40 (2007), pp. 413–416

Loading

[Samarasinghe et al., 2006](#) S.R. Samarasinghe, I. Pastoriza-Santos, M.J. Edirisinghe

Liz-Marzan

Printing gold nanoparticles with an electrohydrodynamic direct-write servi

Gold Bull., 39 (2006), pp. 48–53

Loading

[Sand, 1901](#) H.J.S. Sand

On the concentration at the electrodes in a solution with special reference to the deposition of hydrogen by electrolysis of a mixture of copper sulphate and sulphuric acid

Philol. Mag., 1 (1901), pp. 45–79

Loading

[Schönenberger and Roy, 2005](#) I. Schönenberger, S. Roy

Microscale pattern transfer without photolithography of substrates

Electrochim. Acta, 51 (1) (2005), pp. 809–819

Loading

[Texier et al., 1998](#) F. Texier, L. Servant, J.L. Bruneel, F. Argoul

**in situ probing of interfacial processes in the electrodeposition of copper by
microspectroscopy**

J. Electroanal. Chem., 446 (1998), pp. 189–203

Loading

[Tobias and Hickman, 1965](#) C.W. Tobias, R.G. Hickman

Z. Phys. Chem., 229 (1965), p. 145

Loading

[Tolmachev et al., 1996](#) Y.V. Tolmachev, Z. Wong, D.A. Scherson

**Theoretical aspects of laminar flow in a channel-type electrochemical cell
attenuated total reflection-infrared spectroscopy**

J. Electrochem. Soc., 143 (1996), pp. 3160–3166

Loading

[Wagner, 1949](#) C. Wagner

The role of natural convection in electrolytic processes

Trans. Am. Electrochem. Soc., 95 (1949), p. 61

Loading

[Walton et al., 1995](#) D.J. Walton, S.S. Phull, A. Chyla, J.P. Lorimer, T.J. Mason, L.D.

R.G. Compton, J.C. Eklund, S.D. Page

Sonovoltammetry at platinum electrodes: surface phenomena and mass tr

J. Appl. Electrochem., 25 (1995), pp. 1083–1090

Loading

[Whitaker et al., 2005](#) J.D. Whitaker, J.B. Nelson, D.T. Schwarts

Electrochemical printing: software reconfigurable electrochemical microfi

J. Micromech. MicroEng., 15 (8) (2005), pp. 1498–1503

Loading

[Widayatno and Roy, 2011](#) Widayatno, T., Roy, S., 2011. Electrodeposition of nickel p

photolithography of substrates. In: Proceedings of 3rd International Congress on
Engineering (GPE), Kuala-Lumpur, Malaysia, 6–8 November, 2011.

Loading

[Wragg, 1971](#) A.A. Wragg

Combined free and forced convective ionic mass transfer in the case of open

Electrochim. Acta, 16 (1971), p. 373

Loading

[Wragg and Ross, 1967](#) A.A. Wragg, T.K. Ross

Superposed free and forced convective mass transfer in an electrochemical

Electrochim. Acta, 12 (1967), p. 1421

Loading

[Wu et al., 2011](#) Qi-Bai Wu, T.A. Green, S. Roy

Electrodeposition of microstructures using patterned anode

Electrochem. Commun., 13 (11) (2011), pp. 1229–1232

Loading

[Yeager and Hovorka, 1953](#) E. Yeager, F. Hovorka

Ultrasonic Waves and Electrochemistry. I. A survey of the electrochemical effects of ultrasonic waves

J. Acoust. Soc. Am., 25 (3) (1953), p. 444

Loading

[Yu et al., 2006](#) H. Yu, O. Bologan, B. Li, T.W. Murray, J. Zhang

Fabrication of three-dimensional microstructures based on single-layered microchip applications

Sens. Actuators A, 127 (2006), pp. 228–234

Loading

[Zelinsky and Pirogov, 2009](#) A.G. Zelinsky, B.Y. Pirogov

Electrolysis in a closed Electrochemical cell with a small inter-electrode distance: dissolution/deposition in plain electrolyte

Electrochim. Acta, 54 (2009), pp. 6707–6712

Loading



Corresponding author.

Copyright © 2014 The Authors. Published by Elsevier Ltd.

[About ScienceDirect](#) [Remote access](#) [Shopping cart](#)
[Contact and support](#) [Terms and conditions](#) [Privacy policy](#)

Cookies are used by this site. For more information, visit the [cookies page](#).

Copyright © 2017 Elsevier B.V. or its licensors or contributors. ScienceDirect ® is a registered trademark of Elsevier B.V.

▼ Recommended articles

Assessment of different methods of ana...

2014, Chemical Engineering Science [more](#)

Fibre cross-section determination and v...

2011, Composites Science and Technology [more](#)

Simulation based ionic liquid screenin...

2014, Chemical Engineering Science [more](#)

[View more articles »](#)

▶ Citing articles (12)

▶ Related book content

